Archival Report

Visual Hallucinations Are Characterized by Impaired Sensory Evidence Accumulation: Insights From Hierarchical Drift Diffusion Modeling in Parkinson's Disease

Claire O'Callaghan, Julie M. Hall, Alessandro Tomassini, Alana J. Muller, Ishan C. Walpola, Ahmed A. Moustafa, James M. Shine, and Simon J.G. Lewis

ABSTRACT

BACKGROUND: Models of hallucinations emphasize imbalance between sensory input and top-down influences over perception, as false perceptual inference can arise when top-down predictions are afforded too much precision (certainty) relative to sensory evidence. Visual hallucinations in Parkinson's disease (PD) are associated with lower-level visual and attentional impairments, accompanied by overactivity in higher-order association brain networks. PD therefore provides an attractive framework to explore contributions of bottom-up versus top-down disturbances in hallucinations.

METHODS: We characterized sensory processing during perceptual decision making in patients with PD with ($n = 20$) and without ($n = 25$) visual hallucinations and control subjects ($n = 12$), by fitting a hierarchical drift diffusion model to an attentional task. The hierarchical drift diffusion model uses Bayesian estimates to decompose task performance into parameters reflecting drift rates of evidence accumulation, decision thresholds, and nondecision time.

RESULTS: We observed slower drift rates in patients with hallucinations, which were less sensitive to changes in task demand. In contrast, wider decision boundaries and shorter nondecision times relative to control subjects were found in patients with PD regardless of hallucinator status. Inefficient and less flexible sensory evidence accumulation emerges as a unique feature of PD hallucinators.

CONCLUSIONS: We integrate these results with evidence accumulation and predictive coding models of hallucinations, suggesting that in PD sensory evidence is less informative and may therefore be down-weighted, resulting in overreliance on top-down influences. Considering impaired drift rates as an approximation of reduced sensory precision, our findings provide a novel computational framework to specify impairments in sensory processing that contribute to development of visual hallucinations.

Keywords: Bayesian, Bottom up, Hierarchical drift diffusion model, Parkinson's disease, Perception, Precision, Top down, Visual hallucinations

http://dx.doi.org/10.1016/j.bpsc.2017.04.007

Visual hallucinations (VHs) are common in Parkinson's disease (PD), occurring in over 30% of newly diagnosed and early-stage patients and increasing to upwards of 70% by the late stages of the disease (1–3). However, despite their prevalence, VHs remain poorly understood, and treatment options are limited (4). Continued characterization of the psychological and mechanistic correlates of VHs in PD will be crucial to inform therapeutic advances.

Proposed explanatory models for VHs in PD emphasize a state of reduced sensory input, where the ongoing perceptual process is vulnerable to influence from internally generated imagery (5–8). This is in keeping with a transdiagnostic framework, where hallucinations arise when the balance between sensory input and top-town influence over perception is disrupted, such that sensory information is reduced or not properly integrated, and there is a predominance of top-down influence (9–13). In this context, there is both impairment in sensory evidence accumulation and a failure of Bayesian inference processes regulating top-down versus bottom-up influences on perception.

In formal computational terms, VHs can be considered false perceptual inference (13). Perceptual inference can be computationally implemented by predictive coding or Kalman filtering, in which incoming sensory input is predicted based on past information, and a prediction error specifies the difference between the expected and incoming evidence. Precision is a measure of certainty determining the weight those errors will have (termed their Kalman gain) in influencing the updating of subsequent estimates (14). This is important in theories of hallucinations, where the top-down versus

bottom-up imbalance is driven by a possibly compensatory imbalance of precision, in which top-down predictions are afforded too much precision in relation to sensory evidence. A prediction that follows is that patients with VHs should show reduced sensory precision.

In PD, sensory input is affected by dopaminergic retinal changes and impairments in lower-level visual processes and attention—all of which can be more pronounced in patients with hallucinations (15). However, hallucinations can also occur in patients in whom ophthalmologic measures and performances on lower-level perceptual tasks are equivalent to those in nonhallucinating patients (16). A possibility is that lower-level sensory impairment and reduced attention confer risk factors for VHs in PD, but failures in the dynamic integration of visual input and attention trigger their occurrence (6,8). We aimed to investigate the dynamic processes underlying visual perception in PD hallucinators by applying a drift diffusion model (DDM) to an attentional task. Crucially, attentional deficits (and the use of an attentional task) follow from the above aberrant precision account. In predictive coding, attention serves as a gain control mechanism to enhance the precision of sensory prediction errors (17–21). Increased precision implies more in-depth processing of a stimulus (22). Aberrant precision control is therefore consistent with an attentional deficit, where sensory evidence is not efficiently selected and enhanced, leading to failures in belief updating and perceptual inference.

DDMs are based on the premise that reaction time and response output can be decomposed into parameters reflecting the latent cognitive processes driving task performance (23). The DDM quantifies information extracted from a stimulus (drift rate), the evidence needed to make a decision (boundary separation), and components related to stimulus encoding and response output (nondecision time) (24,25). In the context of predictive coding, the drift rate can be used to approximate precision or Kalman gain, as the rate of sensory evidence accumulation would correspond to the precision (i.e., confidence or certainty) ascribed to the evidence being accumulated. In this study, we applied a Bayesian hierarchical version of the DDM, which is robust in the context of low trial numbers (26,27). This makes the task suitable for clinical contexts where task duration is necessarily limited, and it has been successfully fitted to data from patients with PD in previous studies (28–30). We assessed participants on the attention network task (ANT) (31), which allowed us to measure perceptual decision making under conditions with different levels of difficulty as determined by perceptual conflict in the stimuli.

Under the DDM, we predicted that patients with VHs would show reduced sensory precision relative to patients without hallucinations, as evidenced by impairments in parameters reflecting the integration or accumulation of sensory evidence in the decision-making process, i.e., the drift rate or boundary separation. However, their nondecision components should be similar. We also predicted that control subjects and patients without hallucinations would modulate their drift rate and boundary separation in response to the different levels of perpetual conflict, but that patients with VHs would not show the same level of flexibility in response to task demands.

METHODS AND MATERIALS

Case Selection

We recruited 50 patients from the Parkinson's Disease Research Clinic at the Brain and Mind Centre, University of Sydney. Patients were identified as hallucinators if they self-reported visual hallucinatory phenomena and scored ≥1 on question 2 of the Movement Disorder Society–sponsored revision of the Unified Parkinson's Disease Rating Scale (i.e., over the past week have you seen, heard, smelled or felt things that were not really there? If yes, the examiner asks the patient or caregiver to elaborate and probes for information) (32). This resulted in 24 patients in the VH group and 26 patients in the nonVH group. Four patients from the VH group and 1 from the nonVH group were excluded from analysis owing to excessive missed responses on the experimental task, leaving a final cohort of 20 patients in the VH group and 25 patients in the nonVH group. A proportion of these patients were included in a previous behavioral study of the ANT (33). We recruited 12 age-matched control subjects from a volunteer panel.

All patients satisfied the United Kingdom Parkinson's Disease Society Brain Bank criteria and were not demented, scoring above the recommended Mini-Mental State Examination cutoff of ≥26 (34). Patients were assessed on the Hoehn and Yahr Scale and the Motor Examination section of the Unified Parkinson's Disease Rating Scale. The Mini-Mental State Examination and Montreal Cognitive Assessment were administered as measures of general cognition. Clinical assessments and the experimental task were performed with patients in the "on" state, having taken their regular dopaminergic medication, and dopaminergic dose equivalence scores were calculated. No patients in the cohort were taking antipsychotic medication or cholinesterase inhibitors. Control subjects were screened for a history of neurological or psychiatric disorders. The study was approved by the local ethics committees, and participants provided informed consent.
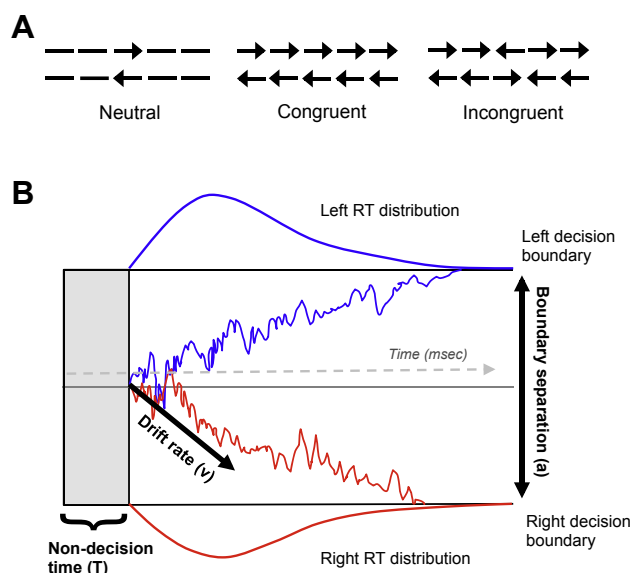
Attention Network Task

We administered a shortened version of the ANT (31), which requires participants to determine if a central arrow points left or right. Central arrows are flanked by flat lines (neutral condition), arrows facing the same direction (congruent condition), or arrows facing a mixture of directions (incongruent condition) (Figure 1A). The perceptual conflict in the incongruent condition is designed to place a greater demand on attentional processes relative to the congruent and neutral conditions. See Supplement for task details.

Hierarchical DDM of the ANT

DDMs are widely applied to rapid, two-choice decision-making tasks such as the ANT (25,35,36). DDMs are typically described by four main parameters: drift rate (v), boundary (a), decision bias (z), and nondecision time (T). The decision process is modeled as the gradual accumulation of information, reflected by the drift rate, which continues until a decision boundary is reached (37). The decision bias parameter captures a priori bias toward one of the two responses. Nondecision time incorporates components that are not part of the evidence accumulation process, including stimulus encoding,

A

Neutral   Congruent   Incongruent

B

Left RT distribution

Left decision
boundary

Time (msec)

Boundary separation (a)

Drift rate (v)

Right decision
boundary

Non-decision
time (T)

Right RT distribution

Figure 1. Attention network task conditions and drift diffusion model. **(A)** The three conditions in the attention network task. Examples of left and right stimulus cues for each condition are shown here; however, in the task, only one cue was presented per trial for a maximum of 1700 ms. **(B)** Schematic example of drift diffusion trajectories. Evidence is noisily accumulated toward a left or right response (blue and red panels), which are separated by the boundary threshold (a). The average evidence accumulation is denoted by drift rate (v). The evidence accumulation begins after a period of nondecision time (T). Density plots show the distribution of observable reaction times (RT). [Adapted from Wiecki *et al.* (26) and Zhang and Rowe (73).]

extracting stimulus dimensions, and executing a response (36). Figure 1B is a schematic diagram of the drift diffusion process. We applied a hierarchical DDM (hDDM) using the hDDM toolbox (http://ski.clps.brown.edu/hddm_docs/) (26). The hDDM uses Bayesian estimation to generate posterior distributions of parameters. This approach optimizes the tradeoff between within-subject and between-subject random effects, accounting for both within-subject variability and group-level similarities, as individual parameters are constrained by a group-level distribution.

We tested three models that all assumed an unbiased starting point (z), given that left/right responses were counterbalanced, and assumed that nondecision time (T) would not be expected to vary as a function of condition, as the stimulus encoding and motor responses required across conditions were comparable. Model specifications were as follows: in the first model, only drift rate (v) was permitted to vary by condition, and decision boundary (a) was held constant; in a second model, decision boundary (a) could vary across conditions, but drift rate (v) was held constant; in a third model, both v and a were free to vary across conditions. For all models, Markov chain Monte Carlo simulations were used to generate 120,000 samples from the joint posterior parameter distribution. The first 20,000 samples were discarded as burn-in, and we used a thinning factor of 10, with outliers specified at 5%. Convergence was assessed by visually inspecting the Markov chains and computing the R-hat Gelman-Rubin statistic where successful coverage is indicated by values <1.1 (37). The best

model was determined by comparing the deviance information criterion (DIC) of each model, which evaluates a model's goodness-of-fit while accounting for model complexity (i.e., number of free parameters), with lower DIC values indicating better model fit (38). To further evaluate the best fitting model, we ran posterior predictive checks by averaging 500 simulations generated from the model's posterior to confirm it could reliably reproduce patterns in the observed data (26). The fitted ANT data and hDDM source code can be found at https://github.com/claireocallaghan/hDDM_ANT_PD.

Statistical Analysis

Independent samples *t* tests and analyses of variance with Tukey post hoc tests compared demographics and behavioral results from the ANT. Parameters from the hDDM were analyzed using Bayesian hypothesis testing to determine the extent of overlap between the percentage of samples drawn from two posterior density distributions. Posterior probabilities are considered significantly different if <5% of the distributions overlap (26–28). The proportion of overlap in the posterior probabilities is denoted by *P* to distinguish it from the classical frequentist *p* values.

RESULTS

Participant Characteristics

The groups were matched for age ($F_{2,54}$ = 1.31, *p* = .28). Performance on the Mini-Mental State Examination was similar across groups ($F_{2,54}$ = 1.07, *p* = .35), but the Montreal Cognitive Assessment revealed significant differences, with the nonVH group performing below the control group ([$F_{2,54}$ = 5.91, *p* < .01]; nonVH group vs. control group, *p* < .01; VH group vs. control and nonVH groups, *p* = .17 and *p* = .19). The patient groups did not differ in disease duration (*t* = −1.42, *p* = .16), Hoehn and Yahr stage (*t* = −1.33, *p* = .19), Unified Parkinson's Disease Rating Scale Motor Examination (*t* = −1.80, *p* = .08), or dopamine dose equivalence (*t* = −1.63, *p* = .11) (Table 1).

Table 1. Demographics and Clinical Characteristics of Patients With Parkinson's Disease and Healthy Control Subjects

	Control Group	PD nonVH Group	PD VH Group
Number	12	25	20
Gender (M:F)	4:8	19:6	15:5
Age, Years	64.75 (5.97)	67.08 (8.22)	68.89 (6.05)
MMSE	29.08 (0.79)	28.39 (1.47)	28.79 (1.72)
MoCA	28.50 (1.45)	26.56 (2.11)	27.41 (1.50)
Disease Duration, Years	—	5.52 (2.86)	7.11 (4.99)
Hoehn and Yahr Stage	—	2.16 (0.47)	2.37 (0.60)
UPDRS III	—	27.67 (11.54)	34.28 (13.97)

Values are mean (SD) or *n*.

F, female; M, male; MMSE, Mini-Mental State Examination; MoCA, Montreal Cognitive Assessment; nonVH, non–visual hallucination; PD, Parkinson's disease; UPDRS III, Unified Parkinson's Disease Rating Scale Motor Examination; VH, visual hallucination.

Visual Hallucinations in PD

ANT Behavioral Results

Participants who made no response on more than one-third of trials were excluded from the study. Trials where no response was made were omitted from the behavioral and modeling analyses, rather than using the upper limit reaction time, which would bias the model. More trials were removed for the VH group compared with the nonVH group, although patients and control subjects did not differ significantly ([$F_{2,54}$ = 4.06, $p < .05$]; control group vs. nonVH and VH groups, $p = .10$ and $p = .09$; VH group vs. nonVH group, $p < .05$).

After removal of no response trials, accuracy was 100% across the three groups. Reaction times are plotted in Figure 2. Global reaction times, regardless of condition, were fastest for the control group followed by the nonVH group and then the VH group, with significant differences evidenced by a main effect for group in the analysis of variance ([$F_{2,162}$ = 8.15, $p < .001$]; VH group vs. control and nonVH groups, both $p < .01$; nonVH group vs. control group, $p = .59$). A main effect of condition revealed that reaction times were significantly slower for the incongruent condition compared with both the congruent and the neutral conditions, whereas the congruent and neutral conductions were equivalent ([$F_{2,162}$ = 17.02, $p < .000001$]; incongruent vs. congruent and neutral, both $p < .00001$; congruent vs. neutral, $p = .98$). There was no significant interaction between group and condition, suggesting that the relatively slowed reaction times for the incongruent condition were consistent across groups ($F_{4,162}$ = 0.04, $p = .99$).

hDDM Fit

All three models showed good convergence (see Supplement for R-hat values). The best-fitting model was model three, which allowed v and a to vary across conditions (DIC model 3 = −636.496, compared with DIC model 1 = −436.160, and

DIC model 2 = −626.593). Posterior predictive checks showed good agreement between the simulated and observed data as shown in Supplemental Figure S1 plotting the observed data against the model prediction. Comparisons showed that the difference between the summary statistics of the simulated and the observed data fell within the 95% credible interval.

Analysis of Model Parameters

Comparisons Between Groups. Figure 3 shows the posterior probability density plots for the drift rate (top panel) and decision boundaries (bottom panel) for the three groups across each condition. The VH group had uniformly lower drift rates compared with the nonVH group; these differed significantly in all conditions (neutral, $P = 0.05\%$; incongruent, $P = 0.04\%$; congruent, $P = 3.41\%$). Drift rates of patients in the VH group were also significantly lower than for control subjects for the incongruent and neutral conditions ($P = 0.04\%$ and $P = 3.43\%$), although not for the congruent condition ($P = 12.72\%$). Posterior probabilities did not differ significantly between nonVH and control groups for any condition (neutral, $P = 84.21\%$; congruent, $P = 66.45\%$; incongruent, $P = 41.19\%$).

For the decision boundary, there were no significant differences between the VH and nonVH groups for any of the conditions (neutral, $P = 31.19\%$; congruent, $P = 50.96\%$; incongruent, $P = 9.45\%$). Both the VH and nonVH groups had significantly larger decision boundaries than the control group in the neutral and congruent conditions (VH group, $P = 0.12\%$ and $P = 0.03\%$; nonVH group, $P = 0.03\%$ and $P = 0.03\%$), and the nonVH group was also significantly larger in the incongruent condition (nonVH group, $P = 0.68\%$; VH group, $P = 14.19\%$). As shown in Figure 4, the VH and nonVH groups had similar nondecision times ($P = 34.04\%$), which were
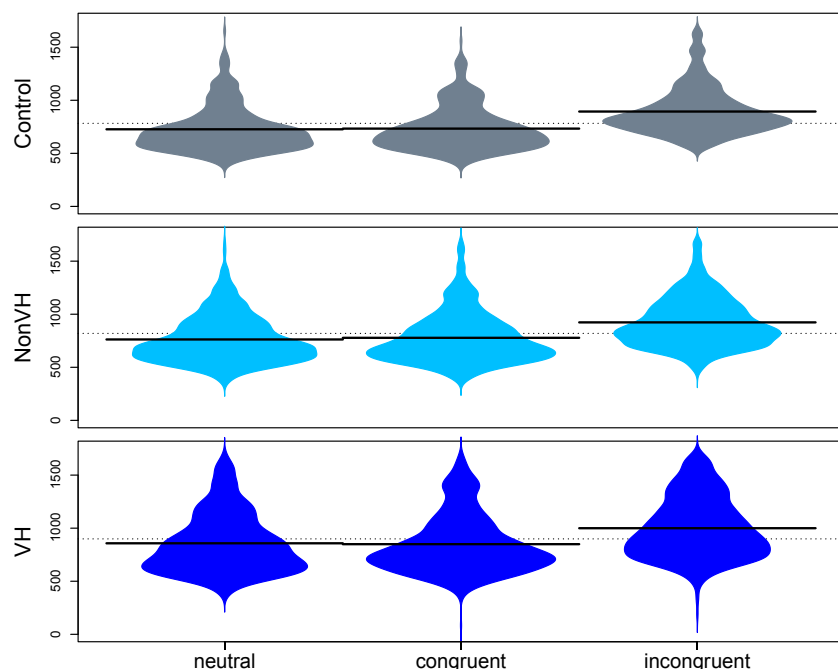
Figure 2. Attention network task reaction times. Reaction time distributions for the attention network task across the three levels of task difficulty. Milliseconds are shown on the y axis. Bold black lines designate the mean reaction times for each condition, and the dotted line shows the overall mean across conditions. The filled colored plots show the density distributions of the reaction times; these are density plots of the data rotated and mirrored symmetrically to show the shape of the data distribution. nonVH, non–visual hallucination; VH, visual hallucination.
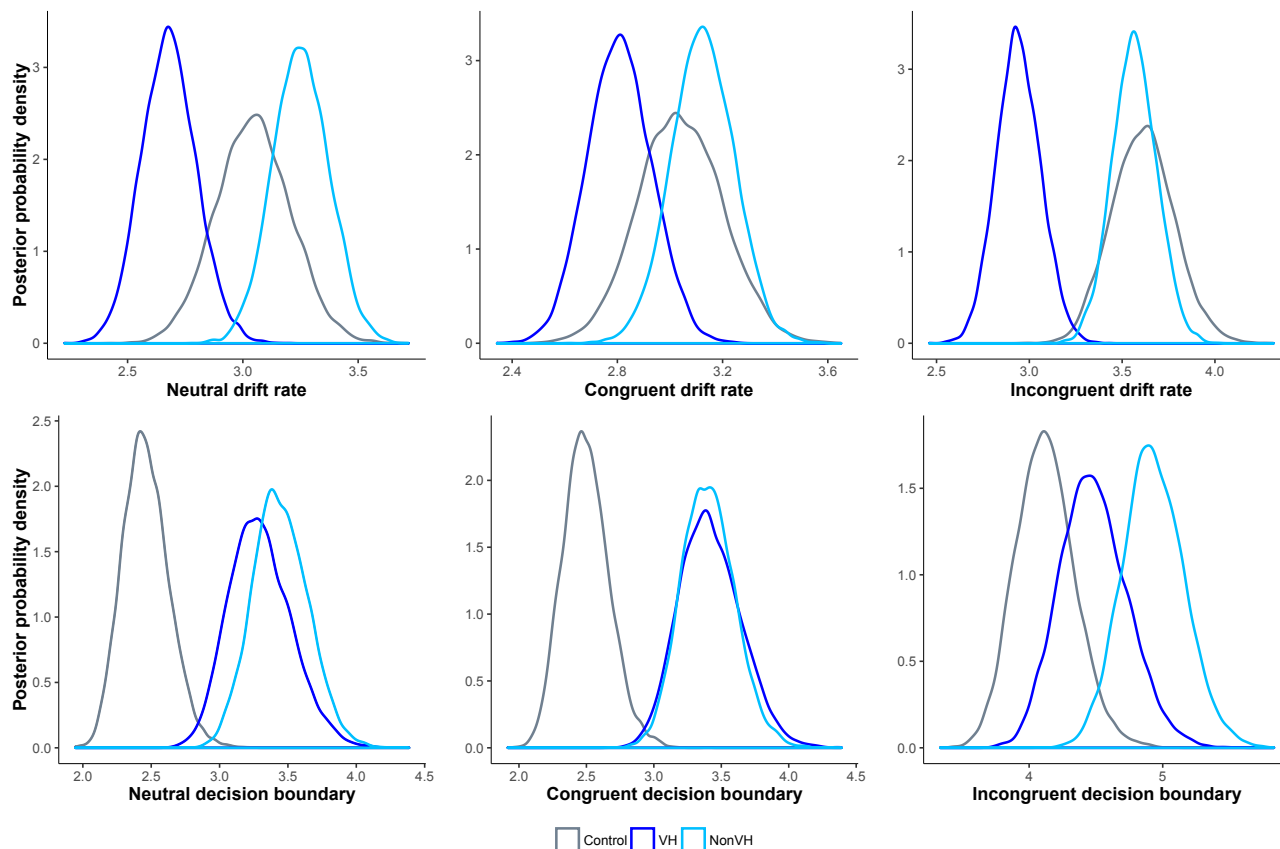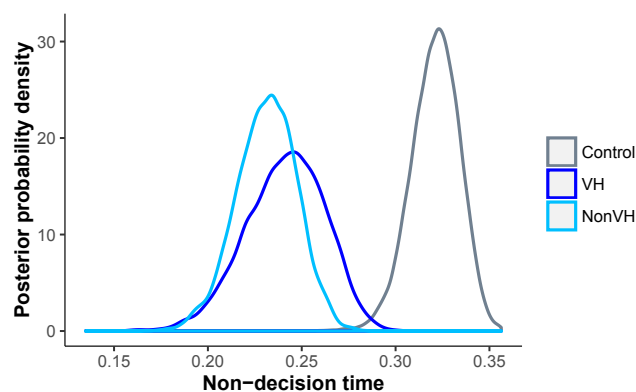
Figure 3. Between-group comparisons of drift rates and decision boundaries. Posterior probability density plots for drift rates (top panel) and decision boundaries (bottom panel). nonVH, non–visual hallucination; VH, visual hallucination.

significantly shorter than the control group (VH group, P = 0.05%; nonVH group, P = 0.00%).

Comparisons Across Conditions. Figure 5 shows posterior probabilities within each group for the three conditions (control group, left panel; nonVH group, middle panel; VH group, right panel). For drift rates, the control group showed an expected pattern with significantly longer drift rates in the
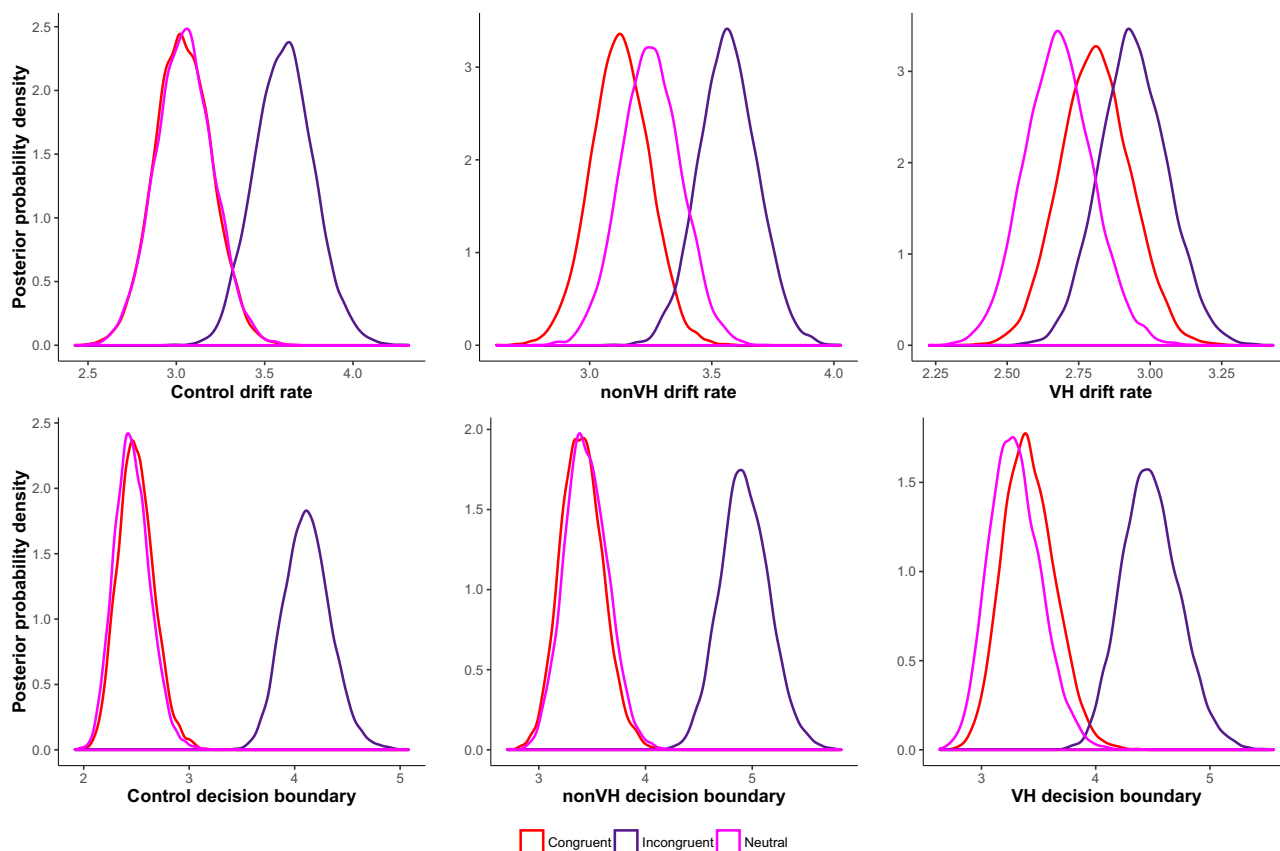

Figure 4. Nondecision time. Posterior probability density plots for nondecision time. nonVH, non–visual hallucination; VH, visual hallucination.

incongruent condition compared with the neutral and congruent conditions (P = 0.28% and P = 0.32%) and similar rates in the neutral and congruent conditions (P = 50.92%). The nonVH group showed a similar pattern with significantly longer drift rates in the incongruent relative to the neutral and congruent conditions (P = 1.55% and P = 0.15%), with similar rates in the neutral and congruent conditions (P = 18.31%). In contrast, compared with the control and nonVH groups, the VH group showed less of a difference between the incongruent and neutral conditions (P = 3.28%) and no significant difference between the incongruent and congruent conditions (P = 17.47%), with similar rates also between neutral and congruent conditions (P = 17.80%). All groups showed a similar pattern for decision boundaries across the conditions, with significantly larger decision boundaries in the incongruent condition relative to the neutral and congruent conditions (control group, P = 0.00% and P = 0.00%; nonVH group, P = 0.00% and P = 0.00%; VH group, P = 0.00% and P = 0.00%), with similar thresholds in the neutral and congruent conditions (control group, P = 38.80%; nonVH group, P = 37.32%; VH group, P = 20.00%).

DISCUSSION

Our results demonstrate two features that characterize the perceptual decision-making process of hallucinating patients

Figure 5. Within-group comparisons of drift rates and decision boundaries. Posterior probability density plots for drift rates (top panel) and decision boundaries (bottom panel). nonVH, non–visual hallucination; VH, visual hallucination.

relative to nonhallucinating patients: lower drift rates and reduced ability to adjust drift rates to accommodate changes in perceptual conflict. Behaviorally, all groups had 100% accuracy on the ANT. Employing a task that patients with PD could easily understand and execute was particularly important, given the possibility of cognitive impairment in this patient cohort. This ensured that we could accurately access perceptual decision making without higher-order cognitive deficits confounding performance. Hallucinating patients had the slowest reaction times on the ANT, although each group showed the expected pattern of shorter reaction times for the easier (neutral and congruent) conditions and longer reaction times for the more difficult (incongruent) condition. Our findings from the hDDM reveal the added benefits of modeling these data to uncover the cognitive processes underlying the behavioral results.

The drift rate reflects how quickly information is accumulated and reflects the quality or precision of evidence that enters the decision-making process (25). In all three conditions, the control and nonVH groups displayed similar drift rates. The VH group had consistently lower drift rates. In between-condition comparisons, drift rates are modulated by task difficulty (24). This effect was apparent in our results for both the control and the nonVH groups. These groups had longer drift rates in the incongruent relative to the congruent

conditions, suggesting that their integration of information into the decision-making process was flexibly modulated in response to imprecise or ambiguous sensory evidence. In contrast, the VH group had similar drift rates across the congruent and incongruent conditions, indicating less flexible context-dependent modulation of sensory accumulation.

Previous work has identified neural correlates of evidence accumulation during perceptual decision making. In monkeys, neuronal populations in sensory areas (e.g., middle temporal visual area) fire in response to properties of a stimulus, and downstream regions (e.g., lateral intraparietal, frontal eye fields, dorsal lateral prefrontal cortex) integrate this information over time until sufficient evidence is accumulated for a decision (39–42). In humans, evidence accumulation has been related to frontoparietal regions [i.e., dorsal and ventrolateral prefrontal cortex and frontal eye fields (43–46)] and the anterior insula (47) as well as integration across large-scale networks (48). In PD, abnormal local and network-level engagement of frontoparietal and insula regions has been found in patients with hallucinations (49–52) and is typically equated with attentional dysfunction. In perceptual decision making, accumulation of sensory evidence and attention are highly collinear—and possibly inseparable—processes (23), consistent with the relationship between attention and sensory precision specified by predictive coding accounts. It follows that

our finding of impaired drift rates may offer a more tangible, computational framework to better specify attentional impairments in patients with PD with VHs.

All groups modulated their decision boundaries in response to the more difficult condition, displaying larger boundaries for the incongruent relative to congruent and neutral conditions. Flexible adaptation of decision thresholds in response to task demands has been shown previously in patients with PD (28,29). Despite the flexible adaptation of thresholds, regardless of hallucination status, patients with PD had larger decision boundaries than control subjects. The lack of difference between the VH and nonVH groups suggests that a widening of decision boundaries during perceptual decision making is a feature of PD more generally. This corresponds to findings in healthy aging, where older adults display wider decision boundaries relative to younger adults (53–55). In older adults, adopting conservative decision criteria is presumed to be a compensatory strategy to prevent errors in speed and/or accuracy tradeoff tasks, and this effect may be amplified in PD.

Hallucinating and nonhallucinating patients also had comparable nondecision times, and these were shorter than times for control subjects. This might have seemed counterintuitive in light of the longer nondecision times shown in aging (56,57), but reduced nondecision times in PD have also been found with the application of an hDDM to a saccadic go/no-go task (30). Nondecision time encompasses diverse processes: encoding evidence from a stimulus and extracting its dimensions to guide the decision-making process and execution of a motor response (36). Decreased latencies in stimulus encoding and extraction of details may drive this finding, or shorter nondecision times may reflect motor impulsivity, which has previously been documented in PD despite general motor slowing (58,59). Future work may make this distinction in PD, although currently nondecision time is a relatively underspecified term compared with the other parameters in the DDM, and few studies have successfully separated its subcomponents (23).

Inefficient and less flexible evidence accumulation during perceptual decision making emerges as a unique feature of hallucinating patients with PD, whereas changes in cautiousness and visuomotor processes are apparent regardless of hallucinator status. Longer drift rate latencies lead to slower decisions, and because perceptual decision making is a noisy process, this increases the chance of errors (37,60). In hallucinating patients with PD, low drift rates that are invariant to changing environmental demands would be a source of low-quality or imprecise information entering the perceptual process.

In terms of aberrant precision control in hallucinating patients with PD, our results are consistent with the simulations reported by Adams et al. (12), namely, an imbalance between sensory precision and the precision of top-down prior beliefs. In PD, there is degeneration of ascending gain-setting neuromodulatory systems (i.e., dopaminergic, cholinergic, and noradrenergic) (61,62) that are associated with implementing precision. Aberrant precision control may be an important unifying principal across PD symptoms. For example, motor symptoms (in particular bradykinesia) may speak to failures in the estimation and attenuation of proprioceptive and somatosensory uncertainty. In active inference accounts, estimating

sensory uncertainty is crucial for initiating movement, as the goal of movement is to reduce the discrepancy between predicted and actual sensory inputs (63,64). Failures of sensory attenuation and compensatory increases in the precision and/or gain at higher levels of processing may underlie both the false inference in VHs and the failure to realize predicted movements in the proprioceptive domain.

Aberrant precision control is ultimately reflected as a failure of Bayesian inference (11,13,65). In a Bayesian framework for perception, sensory input (likelihood) is integrated with known statistics about the environment (priors), forming an estimate of the external stimulus (the posterior). Contributions of the likelihood and prior in generating the posterior estimate are weighted in accordance with their certainty. Noisy or imprecise sensory input is uncertain and carries less weight, shifting the balance in favor of priors. In this context, perception is vulnerable to excessive influence from internally generated beliefs and expectations. In PD, if visual information is accumulated slowly and inefficiently and is therefore less informative, this may contribute to the down weighting of bottom-up information in favor of top-down information.

While the Bayesian framework is a compelling description of hallucinations, it does not necessarily favor a single mechanistic explanation (66). For example, both aberrant predictive coding across hierarchal brain circuitry (67) and large-scale disruptions in the excitatory-to-inhibitory tone of the brain (68) accommodate a Bayesian formulation of hallucinations. Reconciling computational descriptions of hallucinations with a mechanistic framework will open important therapeutic avenues, as predictive coding and excitatory-to-inhibitory accounts rely on distinct neuromodulatory and neurotransmitter profiles. In PD, we are beginning to uncover the psychological and neural signatures associated with a bottom-up versus top-down imbalance in perception. Along with the results of the current study and evidence of lower-level deficits in attention and visual processing, previous work has identified overactivity in the default network of patients with PD with hallucinations (69) and increased coupling between the default network and visual cortex (50). Given the role of the default network in construction of mental imagery (70) and its positioning as a transmodal system distinct from unimodal sensory regions (71), over-engagement of the default network during visual perception may be a source of excessive top-down influence.

Hallucinations develop progressively in PD, beginning with minor illusions before complex hallucinations emerge (4). Patients initially retain full insight into these symptoms, appreciating their occurrence as part of the disease process. With disease progression and cognitive decline, patients can lose insight and develop delusional ideas around the hallucinations. Delusions themselves can be viewed as the instantiation of new priors, to accommodate increasingly noisy or imprecise sensory input (11,72). We employed a limited assessment of hallucinations. Future studies may want to stratify patients in more detail based on the severity and phenomenology of their hallucinations to determine how the imbalance between top-down versus bottom-up influence evolves over the disease course. Additionally, we chose a task manageable for patients with PD; nevertheless, lower-level visual deficits could render such a task more challenging. Future work should employ more detailed visual testing to determine the influence of

low-level vision on sensory evidence accumulation, and replicating the current findings in other perceptual decision-making tasks will be important.

In conclusion, our results suggest that impaired drift rate can be used to approximate precision, providing a novel computational framework encompassing the sensory processing and lower-level attentional deficits previously described in individuals with VHs. Alterations in the dynamic process of sensory evidence accumulation may therefore be a valuable marker to exploit in future explanatory and therapeutic studies of PD VHs.

ARTICLE INFORMATION

From the Department of Psychiatry and Behavioural and Clinical Neuroscience Institute (CO) and Department of Clinical Neurosciences and Cognition and Brain Sciences Unit (AT), University of Cambridge, Cambridge, United Kingdom; Brain and Mind Centre (CO, JMH, AJM, ICW, JMS, SJGL), University of Sydney; School of Social Sciences and Psychology (JMH, AAM), Western Sydney University, Sydney, Australia; and School of Psychology (JMS), Stanford University, Palo Alto, California.

Address correspondence to Claire O'Callaghan, Ph.D., Herchel Smith Building for Brain & Mind Sciences, Cambridge Biomedical Campus, Cambridge CB2 0SZ, UK; E-mail: co365@cam.ac.uk.

REFERENCES

1. Hely MA, Reid WG, Adena MA, Halliday GM, Morris JG (2008): The Sydney multicenter study of Parkinson's disease: The inevitability of dementia at 20 years. Mov Disord 23:837–844.
2. Pagonabarraga J, Martinez-Horta S, Fernández de Bobadilla R, Pérez J, Ribosa-Nogué R, Marín J, et al. (2016): Minor hallucinations occur in drug-naive Parkinson's disease patients, even from the premotor phase. Mov Disord 31:45–52.
3. Holroyd S, Currie L, Wooten G (2001): Prospective study of hallucinations and delusions in Parkinson's disease. J Neurol Neurosurg Psychiatry 70:734–738.
4. Ffytche DH, Creese B, Politis M, Chaudhuri KR, Weintraub D, Ballard C, et al. (2017): The psychosis spectrum in Parkinson disease. Nat Rev Neurol 13:81–95.
5. Shine JM, O'Callaghan C, Halliday GM, Lewis SJG (2014): Tricks of the mind: Visual hallucinations as disorders of attention. Prog Neurobiol 116:58–65.
6. Collerton D, Perry E, McKeith I (2005): Why people see things that are not there: A novel perception and attention deficit model for recurrent complex visual hallucinations. Behav Brain Sci 28:737–757.
7. Hobson JA, Pace-Schott EF, Stickgold R (2000): Dreaming and the brain: Toward a cognitive neuroscience of conscious states. Behav Brain Sci 23:793–842.
8. Diederich NJ, Goetz CG, Stebbins GT (2005): Repeated visual hallucinations in Parkinson's disease as disturbed external/internal perceptions: Focused review and a new integrative model. Mov Disord 20:130–140.
9. O'Callaghan C, Kveraga K, Shine JM, Adams RB Jr, Bar M (2017): Predictions penetrate perception: Converging insights from brain, behaviour and disorder. Conscious Cogn 47:63–74.
10. Powers AR, Kelley M, Corlett PR (2016): Hallucinations as top-down effects on perception. Biol Psychiatry Cogn Neurosci Neuroimaging 1:393–400.
11. Fletcher PC, Frith CD (2009): Perceiving is believing: A Bayesian approach to explaining the positive symptoms of schizophrenia. Nat Rev Neurosci 10:48–58.
12. Adams RA, Stephan KE, Brown HR, Frith CD, Friston KJ (2013): The computational anatomy of psychosis. Front Psychiatry 4:47.
13. Friston KJ (2005): Hallucinations and perceptual inference. Behav Brain Sci 28:764–766.
14. Rao RP (1999): An optimal estimation approach to visual perception and learning. Vision Res 39:1963–1989.
15. Weil RS, Schrag AE, Warren JD, Crutch SJ, Lees AJ, Morris HR (2016): Visual dysfunction in Parkinson's disease. Brain 139:2827–2843.
16. Gallagher DA, Parkkinen L, O'Sullivan SS, Spratt A, Shah A, Davey CC, et al. (2011): Testing an aetiological model of visual hallucinations in Parkinson's disease. Brain 134:3299–3309.
17. Rao RP (2005): Bayesian inference and attentional modulation in the visual cortex. Neuroreport 16:1843–1848.
18. Spratling MW (2008): Predictive coding as a model of biased competition in visual attention. Vision Res 48:1391–1408.
19. Feldman H, Friston K (2010): Attention, uncertainty, and free-energy. Front Humn Neurosci 4:215.
20. Jiang J, Summerfield C, Egner T (2013): Attention sharpens the distinction between expected and unexpected percepts in the visual brain. J Neurosci 33:18438–18447.
21. Friston KJ, Stephan KE (2007): Free-energy and the brain. Synthese 159:417–458.
22. Wiese W, Metzinger TK (2017): Vanilla PP for philosophers: A primer on predictive processing. In: Metzinger TK, Wiese W, editors. Philosophy and Predictive Processing. Frankfurt am Main: MIND Group.
23. Mulder M, Van Maanen L, Forstmann B (2014): Perceptual decision neurosciences—a model-based review. Neuroscience 277:872–884.
24. Voss A, Rothermund K, Voss J (2004): Interpreting the parameters of the diffusion model: An empirical validation. Mem Cognit 32:1206–1220.
25. Ratcliff R, McKoon G (2008): The diffusion decision model: Theory and data for two-choice decision tasks. Neural Comput 20:873–922.
26. Wiecki TV, Sofer I, Frank MJ (2013): HDDM: Hierarchical bayesian estimation of the drift-diffusion model in python. Front Neuroinform 7:14.
27. Cavanagh JF, Wiecki TV, Kochar A, Frank MJ (2014): Eye tracking and pupillometry are indicators of dissociable latent decision processes. J Exp Psychol Gen 143:1476.
28. Herz DM, Zavala BA, Bogacz R, Brown P (2016): Neural correlates of decision thresholds in the human subthalamic nucleus. Curr Biol 26:916–920.
29. Cavanagh JF, Wiecki TV, Cohen MX, Figueroa CM, Samanta J, Sherman SJ, et al. (2011): Subthalamic nucleus stimulation reverses mediofrontal influence over decision threshold. Nat Neurosci 14:1462–1467.
30. Zhang J, Rittman T, Nombela C, Fois A, Coyle-Gilchrist I, Barker RA, et al. (2016): Different decision deficits impair response inhibition in progressive supranuclear palsy and Parkinson's disease. Brain 139:161–173.
31. Fan J, McCandliss BD, Sommer T, Raz A, Posner MI (2002): Testing the efficiency and independence of attentional networks. J Cogn Neurosci 14:340–347.
32. Goetz CG, Tilley BC, Shaftman SR, Stebbins GT, Fahn S, Martinez-Martin P, et al. (2008): Movement Disorder Society-sponsored revision of the Unified Parkinson's Disease Rating Scale (MDS-UPDRS): Scale presentation and clinimetric testing results. Mov Disord 23:2129–2170.
33. Hall JM, O'Callaghan C, Shine JM, Muller AJ, Phillips JR, Walton CC, et al. (2016): Dysfunction in attentional processing in patients with Parkinson's disease and visual hallucinations. J Neural Transm (Vienna) 123:503–507.

34. Martinez-Martin P, Falup-Pecurariu C, Rodriguez-Blazquez C, Serrano-Dueñas M, Carod Artal F, Rojo Abuin J, et al. (2011): Dementia associated with Parkinson's disease: Applying the Movement Disorder Society Task Force criteria. Parkinsonism Relat Disord 17:621–624.

35. Wagenmakers E-J (2009): Methodological and empirical developments for the Ratcliff diffusion model of response times and accuracy. Eur J Cogn Psychol 21:641–671.

36. Ratcliff R, Smith PL, Brown SD, McKoon G (2016): Diffusion decision model: Current issues and history. Trends Cogn Sci 20:260–281.

37. Krypotos A-M, Beckers T, Kindt M, Wagenmakers E-J (2015): A Bayesian hierarchical diffusion model decomposition of performance in Approach-Avoidance Tasks. Cogn Emot 29:1424–1444.

38. Spiegelhalter DJ, Best NG, Carlin BP, Van Der Linde A (2002): Bayesian measures of model complexity and fit. J R Stat Soc Series B Stat Methodol 64:583–639.

39. Newsome WT, Britten KH, Movshon JA (1989): Neuronal correlates of a perceptual decision. Nature 341:52–54.

40. Gold JI, Shadlen MN (2001): Neural computations that underlie decisions about sensory stimuli. Trends Cogn Sci 5:10–16.

41. Shadlen MN, Newsome WT (2001): Neural basis of a perceptual decision in the parietal cortex (area LIP) of the rhesus monkey. J Neurophysiol 86:1916–1936.

42. Heekeren HR, Marrett S, Ungerleider LG (2008): The neural systems that mediate human perceptual decision making. Nat Rev Neurosci 9:467–479.

43. Heekeren HR, Marrett S, Bandettini PA, Ungerleider LG (2004): A general mechanism for perceptual decision-making in the human brain. Nature 431:859–862.

44. Heekeren HR, Marrett S, Ruff DA, Bandettini P, Ungerleider LG (2006): Involvement of human left dorsolateral prefrontal cortex in perceptual decision making is independent of response modality. Proc Natl Acad Sci 103:10023–10028.

45. Liu T, Pleskac TJ (2011): Neural correlates of evidence accumulation in a perceptual decision task. J Neurophysiol 106:2383–2398.

46. Philiastides MG, Sajda P (2007): EEG-informed fMRI reveals spatio-temporal characteristics of perceptual decision making. J Neurosci 27:13082–13091.

47. Ho TC, Brown S, Serences JT (2009): Domain general mechanisms of perceptual decision making in human cortex. J Neurosci 29:8675–8687.

48. Shine JM, Bissett PG, Bell PT, Koyejo O, Balsters JH, Gorgolewski KJ, et al. (2016): The dynamics of functional brain networks: Integrated network states during cognitive task performance. Neuron 92:544–554.

49. Goetz CG, Vaughan CL, Goldman JG, Stebbins GT (2014): I finally see what you see: Parkinson's disease visual hallucinations captured with functional neuroimaging. Mov Disord 29:115–117.

50. Shine JM, Muller AJ, O'Callaghan C, Hornberger M, Halliday GM, Lewis SJG (2015): Abnormal connectivity between the default mode and the visual system underlies the manifestation of visual hallucinations in Parkinson's disease: A task-based fMRI study. NPJ Parkinsons Dis 1:15003.

51. Stebbins G, Goetz C, Carrillo M, Bangen K, Turner D, Glover G, et al. (2004): Altered cortical visual processing in PD with hallucinations: An fMRI study. Neurology 63:1409–1416.

52. Ramírez-Ruiz B, Martí MJ, Tolosa E, Falcón C, Bargalló N, Valldeoriola F, et al. (2008): Brain response to complex visual stimuli in Parkinson's patients with hallucinations: A functional magnetic resonance imaging study. Mov Disord 23:2335–2343.

53. Ratcliff R, Thapar A, McKoon G (2007): Application of the diffusion model to two-choice tasks for adults 75-90 years old. Psychol Aging 22:56.

54. Spaniol J, Madden DJ, Voss A (2006): A diffusion model analysis of adult age differences in episodic and semantic long-term memory retrieval. J Exp Psychol Learn Mem Cogn 32:101.

55. Ratcliff R, Thapar A, McKoon G (2001): The effects of aging on reaction time in a signal detection task. Psychol Aging 16:323.

56. Starns JJ, Ratcliff R (2010): The effects of aging on the speed-accuracy compromise: Boundary optimality in the diffusion model. Psychol Aging 25:377.

57. Ratcliff R (2008): Modeling aging effects on two-choice tasks: Response signal and response time data. Psychol Aging 23:900.

58. O'Callaghan C, Naismith SL, Hodges JR, Lewis SJG, Hornberger M (2013): Fronto-striatal atrophy correlates of inhibitory dysfunction in Parkinson's disease versus behavioural variant frontotemporal dementia. Cortex 49:1833–1843.

59. Nombela C, Rittman T, Robbins TW, Rowe JB (2014): Multiple modes of impulsivity in Parkinson's disease. PLoS One 9:e85747.

60. Herz DM, Bogacz R, Brown P (2016): Neuroscience: Impaired decision-making in Parkinson's disease. Curr Biol 26:R671–R673.

61. Del Tredici K, Rüb U, De Vos RA, Bohl JR, Braak H (2002): Where does Parkinson disease pathology begin in the brain? J Neuropathol Exp Neurol 61:413–426.

62. Surmeier DJ, Obeso JA, Halliday GM (2017): Selective neuronal vulnerability in Parkinson disease. Nat Rev Neurosci 18:101–113.

63. Friston K, Mattout J, Kilner J (2011): Action understanding and active inference. Biol Cybern 104:137–160.

64. Palmer C, Zapparoli L, Kilner JM (2016): A new framework to explain sensorimotor beta oscillations. Trends Cogn Sci 20:321–323.

65. Corlett P, Frith CD, Fletcher P (2009): From drugs to deprivation: A Bayesian framework for understanding models of psychosis. Psychopharmacology 206:515–530.

66. Teufel C, Fletcher PC (2016): The promises and pitfalls of applying computational models to neurological and psychiatric disorders. Brain 139:2600–2608.

67. Friston KJ, Stephan KE, Montague R, Dolan RJ (2014): Computational psychiatry: The brain as a phantastic organ. Lancet Psychiatry 1:148–158.

68. Jardri R, Hugdahl K, Hughes M, Brunelin J, Waters F, Alderson-Day B, et al. (2016): Are hallucinations due to an imbalance between excitatory and inhibitory influences on the brain? Schizophr Bull 42:1124–1134.

69. Franciotti R, Delli Pizzi S, Perfetti B, Tartaro A, Bonanni L, Thomas A, et al. (2015): Default mode network links to visual hallucinations: A comparison between Parkinson's disease and multiple system atrophy. Mov Disord 30:1237–1247.

70. Andrews-Hanna JR (2012): The brain's default network and its adaptive role in internal mentation. Neuroscientist 18:251–270.

71. Margulies DS, Ghosh SS, Goulas A, Falkiewicz M, Huntenburg JM, Langs G, et al. (2016): Situating the default-mode network along a principal gradient of macroscale cortical organization. Proc Natl Acad Sci U S A 113:12574–12579.

72. Corlett PR, Fletcher PC (2015): Delusions and prediction error: Clarifying the roles of behavioural and brain responses. Cogn Neuropsychiatry 20:95–105.

73. Zhang J, Rowe JB (2014): Dissociable mechanisms of speed-accuracy tradeoff during visual perceptual learning are revealed by a hierarchical drift-diffusion model. Front Neurosci 8:69.